

H₃S is a high- κ superconductor with columnar pinning defects

Miodrag L. Kulić

Institute for Theoretical Physics, Goethe-University Frankfurt am Main, Germany

(Dated: February 13, 2023)

Recently, the existence of superconductivity in H₃S and other high-pressure hydrides is called into question, because of some flawed magnetic measurements. In Ref. [1]) the SCPC model is proposed, where strong pinning of vortices is due to long columnar defects in H₃S - with lengths L of the order of vortex lengths L_v . Two relevant type of experiments in magnetic fields are explained by this model: (1) Reduction (with respect to standard superconductors) of the thermal broadening of resistance (TBR) in magnetic field $h = H/H_{c2}$, $\delta t_c(h)$, is governed by the small parameter $C = \xi_0/L$, i. e. $\delta t_c^{scpc}(h) \sim C^{1/2}h^{1/2}$ with $C \sim 10^{-3}$. This gives $\delta t_c^{scpc}(h) \lesssim 0.01$ for $h \lesssim 0.01$ and $L \sim 1 \mu m$, which is in satisfactory agreement with measurements in H₃S [2]. The TBR measurements give, that in H₃S there is a large shift of the irreversible line $B_{irr}(T)$ towards the $B_{c2}(T)$ line, with $B_{irr}^{(H_3S)} \sim C^{-1}(1-t)^2$ instead of $B_{ir} \sim (1-t)^{3/2}$ ($t = T/T_c$) - in standard superconductors with point defects. (2) In ZFC (zero field cooled) experiments on penetration of the magnetic field (PMF) in H₃S [3], the latter reaches the center of a superconducting disk at much larger external fields, i. e. for $B_0 \gg B_{c1}$. The later is due to the pronounced pinning of vortices, but not to the Meissner effect. The calculated T - dependence of the penetrated, perpendicular $B_{\perp}(T)$ and parallel $B_{\parallel}(T)$, magnetic field into the sample is in satisfactory agreement with the experimental results for H₃S in [3], where $B_{\perp} > B_{\parallel}$. Problems related to measurements of the Meissner effect in H₃S are also discussed. The SCPC model, applied on the measurements in the bulk H₃S sample, predicts, that the latter is a high- κ superconductor with $\xi_0 \approx (15 - 20) \text{ \AA}$, $\lambda_0 \approx (1 - 2) \times 10^3 \text{ \AA}$; $\kappa \approx (50 - 100)$, $\mu_0 H_{c1}(0) \approx (18 - 60) \text{ mT}$, $\mu_0 H_{c0} \approx (0, 6 - 1, 1) \text{ T}$, $\mu_0 H_{c2}(0) \approx (80 - 140) \text{ T}$.

I. INTRODUCTION

The first almost room-temperature superconductor was reported in 2015 in sulphur-hydrides (H_3S) with $T_c \approx 203 \text{ K}$ under high pressure $P \approx 150 \text{ GPa}$ ($\approx 1.5 \text{ Mbar}$), which is based on resistivity measurements [4]. This finding opens a new frontier in physics and a number of other HP-hydrides were predicted before these were synthesized thereafter. Let us mention some of them with $T_c \geq 200 \text{ K}$ - such as LaH₁₀ with $T_c \approx 250 \text{ K}$, $P \approx 190 \text{ GPa}$ [5]; LaYH_x with $T_c = 253 \text{ K}$, $P \approx 190 \text{ GPa}$ [6]. In all of them T_c goes down by increasing magnetic field, compatible with the standard theory of superconductivity. There are also reports on the room temperature superconductivity in the CSH hydride - a superconductor based on C, S and H, with $T_c = 287 \text{ K}$ at $P \approx 267 \text{ GPa}$ [7]. However, this result was not yet confirmed, neither experimentally nor theoretically by other groups.

There is also theoretical support for the (almost) room-temperature superconductivity in HP-hydrides, which are based on the calculated critical temperature T_c in the microscopic Migdal-Eliashberg theory for superconductivity - which is due to the electron-phonon interaction. Moreover, the theoretical prediction of superconductivity in HP-hydrides [8] is a rare example in the physics of superconductivity, that the theory goes ahead of experiments, by predicting T_c ($\approx 200 \text{ K}$) in H₃S. Note, that in [4] the H₂S structure is proposed, while in [9] it is argued, that at high pressures the phase diagram favors decomposition of H₂S into H₃S and pure S.

A main proof for superconductivity is the existence of the Meissner effect, where the magnetic field $H < H_{c1}$ - applied above T_c , is *expelled* from the sample at tem-

peratures below T_c - the field cooled (FC) experiment. However, until now the Meissner effect is not proved experimentally in HP-hydrides, which caused justified criticism on this subject in [10]-[13]. The failure to measure the Meissner effect in H₃S is due to the following reasons: (i) Magnetic measurements in small samples are delicate; (ii) The existence of some extrinsic paramagnetic effects in samples. In that respect, some contradictory experimental results and their inconsistent theoretical interpretations - given in [2],[4],[14], were among the reasons that Hirsch and Marsiglio even called into question the existence of superconductivity in HP-hydrides [10]-[13]. In the following, we are going to show that some magnetic measurements in HS can refute this skepticism.

The content of the article is following. In Section II the SCPC model - firstly introduced in [1] for hard type-II superconductors with strong columnar pinning centers, is further elaborated and applied to the magnetic measurements in the H₃S superconductor. This model proposes, that the vortex pinning is due to long columnar defects ($L \sim L_v \gg \xi_0$) - with the radius of the cross-section $r \sim \xi_0$. In that case, the core and electromagnetic pinning contribute almost equally to the elementary pinning energy U_p . This is an optimal situation for pinning in a superconductor, since there is a maximal gain in the condensation and electromagnetic vortex energy. This gives a maximal pinning force if the superconductivity is fully suppressed in the columnar defects, i.e. for $\Delta = 0$ inside a defect. It seems that Δ is finite in H₃S, but ($\Delta < \Delta_0$) and the critical current density is smaller than the maximal one, i.e. $j_{co} = \eta_{col} j_{c0}^{\max}$ with $\eta_{col} < 1$. In Section III the reduction of the temperature broadening of resistance (TBR) in a magnetic field, $\delta t_c^{exp}(h)$ (with $h = H/H_{c2}$),

in HP-hydrides is studied in the SCPC model and applied to H_3S . The temperature dependence of the irreversibility line with $B_{ir} \sim C^{-1}(1-t)^2$ is predicted within the SCPC model also in Section III. In Section IV the SCPC model is applied in studying the penetration of the magnetic field (*PMF*) into the center of the H_3S sample. The *PMF* measurements are analyzed in the Bean critical state model, first for a long superconducting cylinder (the parallel configuration B_{\parallel} approximately realized in [3]) and then for thin disks (perpendicular configuration B_{\perp}). It is shown, that the critical magnetic field B_p at which it penetrates into the center of the sample is larger for the perpendicular geometry than for the parallel one, i.e. $B_{p\perp} > B_{p\parallel}$. The comparison of the theory and the experimental results for *PMF* in H_3S [3] gives a large critical current $j_{c0} \gtrsim 10^7$ A/cm².

In Section IV we discuss some experimental controversies related to the Meissner effect and FC experiments in H_3S , which display a large residual paramagnetic magnetization. The latter fact does not fit into the classical theory of the Meissner effect. Note, that the paramagnetic signal can be present in some magnetic superconductors, superconductors with intrinsic magnetic moments in [15]-[16] or extrinsic ones [17]. Finally, in Section V the obtained results for TBR and *PMF* in the SCPC model for H_3S are summarized and discussed. Here, the crucial difference between pinning forces in HTSC-cuprates and HP-hydrides is also discussed. Note, in the following we use the notation $\xi_0 \approx \xi(T \ll T_c)$ and $\lambda_0 \approx \lambda(T \ll T_c)$

II. STRONG VORTEX PINNING BY COLUMNAR DEFECTS IN H_3S

A. Single vortex pinning

To increase the critical current density it is desirable to have extended (long columnar) pinning defects - the *correlated disorder*. In this case the pinning potential is correlated over the extended size of the defect $L \sim L_v$. (L_v is the vortex length.) This means that the superconductivity is suppressed in a large volume $V_{col} = \pi \xi_0^2 L_v$ and therefore a single vortex prefers sitting on this defect. Note, that the maximal pinning energy $U_p^{max} = \epsilon_p^{max} V_{col}$ is reached when the superconductivity is fully suppressed in the core of defects, i.e. when $\Delta = 0$ in dielectric columnar defects. This might be not the case in H_3S , where the real pinning energy density is $\epsilon_p = \eta_{col} \cdot \epsilon_p^{max}$ with the reducing factor $\eta_{col} < 1$, because the gap inside the columnar defect is finite, $\Delta < \Delta_0$. In that case $\eta_{col} = \epsilon_p / \epsilon_p^{max} \sim (1 - \Delta^2 / \Delta_0^2)$. As a result, the critical current density for a single vortex (sitting on such a defect) is given by $j_c = \eta_{col} \cdot j_c^{max}$.

Note, that in HTSC-cuprates long columnar pinning defects are made artificially by irradiating $YBa_2Cu_3O_7$ single crystalline samples of small platelets of $1 \times 1 \times 0.02$ mm³ with different doses of 580 MeV $^{116}Sn^{30+}$ ions [18]-[19]. The density of the ion doses are $D \approx 5 \times 10^{10}, 1.5 \times$

$10^{11}, 2.4 \times 10^{11}$ ions/cm², which are equivalent to the corresponding vortex densities with the magnetic induction $B_{\phi} \approx 1, 3, 5$ T - B_{ϕ} is the matching field. Since the ionization energy-loss rate was 2.7 keV/Å they produce long tracks with the length $L \sim 20 - 30 \mu m$ and diameter ~ 50 Å. In that case $j_c (\sim j_{c0})$ is of the order 1.5×10^7 A/cm² at $T = 5$ K and 10^6 A/cm² at $T = 77$ K. These current densities are much larger than those for point defects, where the pinning is due to oxygen vacancies. In the columnar case the irreversible line $B_{ir}(T)$ (the line below which the pinning is pronounced) lies higher than for weak pinning with point defects [18].

In the following it is argued, that the columnar pinning defects dominate in H_3S - see blue colored cylinders in *Fig. 2*, with the averaged distance $d_{\phi} = (\Phi_0 / B_{\phi})^{1/2}$ [20]-[21]. For an optimal pinning the superconductivity should be fully destroyed inside the dielectric columnar defect with radius $r \gtrsim \xi$ [20]-[21]. In this case, both mechanisms of pinning - the *core* and the *electromagnetic* one, are operative with almost same pinning energy [21]. The maximal pinning energy is given by $U_p^{scpc} \approx 2\pi \xi^2 L_v (H_c^2 / 8\pi) \equiv L_v \epsilon_p^{max}$ with $\epsilon_p^{max} \approx \Phi_0^2 / 32\pi^2 \lambda^2(T)$. Since the elementary pinning force (per unit vortex length) $f_p = \epsilon_p^{max} / \xi$ is balanced in the critical state by the Lorenz force (per unit length) $f_L (\equiv F_L / L_v) = j_c \Phi_0 / c$, the critical current density j_c^{max} in the SCPC model is given by [20]-[21]

$$j_c^{max} \approx \frac{c\Phi_0}{32\pi^2 \lambda^2 \xi}. \quad (1)$$

In anisotropic superconductors j_c^{max} is given in [21]. (In SI units $j_{c,SI}^{max} \approx \Phi_0 / 8\pi\mu_0 \lambda^2 \xi$, where $\lambda(T) \approx \lambda_0(1-t)^{-1/2}$ and $\xi(T) \approx \xi_0(1-t)^{-1/2}$ are the Ginzburg-Landau penetration depth and coherence length, respectively). In H_3S one has $\lambda \approx (1-2) \times 10^3$ Å and $\xi_0 \sim (15-20)$ Å [4], which gives for j_c^{max} in the range $j_{c0}^{max} \approx (0.8-3) \times 10^8$ A/cm². In the following, the critical current density j_{c0} will be estimated from experiments on the magnetic penetration in H_3S [3], where it is found $j_{c0} \approx (1, 3 - 1, 5) \times 10^7$ Å/cm², which gives for the reducing factor $\eta \approx (0.1 - 0, 3)$.

B. Crossover field B_{tb} for the single vortex to vortex bundles pinning

The generic $H - T$ phase diagram for the high temperature superconductors with columnar pinning defects is shown in *Fig. 1* - see [19], and some magnetic properties of H_3S will be discussed in the framework of this phase diagram. In **II.B** the single-vortex pinning is considered, which occurs at small magnetic field $B < B_{\phi}$. When the inter-vortex distance $a_v \approx (\Phi_0 / B)^{1/2}$ is larger than the average distance between columnar defects $d_{\phi} = (\Phi_0 / B_{\phi})^{1/2}$ and the single vortex pinning energy is larger than the inter-vortex energy, than the vortices accommodate freely to the pinning sites. However, when $B > B_{\phi}$ the inter-vortex interaction starts to be important for pinning and dynamical properties (such as the

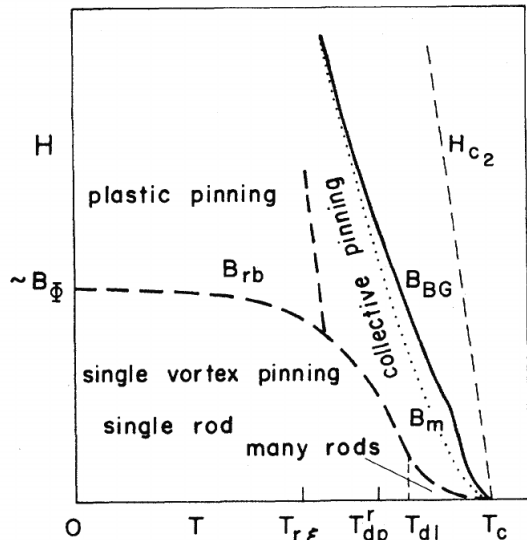


FIG. 1: The generic $H - T$ phase diagram for superconductors with *columnar defects*. The dotted melting line $B_m(T)$ of the pure sample is transformed into a Bose-glass transition line $B_{BG}(T)$. Also shown are the various pinning regimes with a single-vortex/single-rod pinning region at low fields $\mu_0 H < B_{rb}(T) < 2B_\Phi$. For $T < T_{dp}^r$ the fluctuations of a vortex from one defect to another are suppressed, while for $T > T_{dp}^r$ the pinning potential is exponentially reduced. At $T > T_{dl}$ the individual flux lines are pinned collectively by an assembly of columnar defects (rods) at high temperatures. Above the crossover line $B_{rb}(T)$, the largest energy in the problem is the inter-vortex interaction and pinning involves vortex bundles - taken from [19].

vortex creep). In that case, vortex bundles are pinned. The maximal crossover field B_{rb}^{\max} - see *Fig. 1*, separates the single vortex regime from the vortex bundle regime and it is obtained by comparing the energy of the elastic shear deformation (of the order $u \sim d_\Phi$) with the maximal pinning potential ϵ_p^{\max} per unit length, i.e. $\epsilon_{\text{shear}} = c_{66}(d_\Phi/a_v)^2 a_v^2 \simeq \epsilon_p^{\max}$. The shear modulus is given by $c_{66} \approx \Phi_0 B / (8\pi\lambda)^2$ what gives for B_{rb}

$$B_{rb} < B_{rb}^{\max} \lesssim \frac{4\epsilon_p^{\max}}{\epsilon_0} B_\Phi, \quad (2)$$

where $\epsilon_0 = \Phi_0^2 / 16\pi^2 \lambda^2$ [19]. Since $\epsilon_p^{\max} = \epsilon_0 / 2$ it gives, that for $B < B_{br} < B_{rb}^{\max} \approx 2B_\Phi$ the columnar defects outnumber the vortices and the single-vortex pinning prevails. Note, that the real crossover field is $B_{rb} < B_{rb}^{\max}$. Since, $\eta_{\text{col}} < 1$ this inequality holds for $T \ll T_c$, where $\xi(T) \approx \xi_0$ and $\lambda(T) \approx \lambda_0$. It is argued below, that in order to explain the TBR experiment in H_3S the regime $B > B_{rb}$ is also realized.

Note, that in cuprates with columnar defects, pinning properties are highly anisotropic with the maximal critical current for the magnetic field aligned along the columnar defect (and for $j_c \perp \mathbf{H}$). The latter is confirmed for

irradiated $\text{YBa}_2\text{Cu}_3\text{O}_7$ [18]. It seems, that this is not the case for H_3S , where $j_{c0}^\perp \approx j_{c0}^\parallel$ and similar columnar densities of defects are realized along and perpendicular to the sample surface, i. e. $B_\Phi^\perp \simeq B_\Phi^\parallel$ [3]. This implies that the columnar defects in H_3S are oriented along, both, perpendicular and parallel, axes almost equally - see *Fig. 2*.

C. Thermal vortex depinning from columnar defects

For any high temperature superconductor thermal fluctuations of vortex lines are important at higher temperatures, because of smoothing of the pinning potential. This significantly lowers $j_c(T)$ at and above some depinning temperature T_{dp}^r , when the effective pinning potential (per unit vortex length) $\epsilon_p(T) = \epsilon_p(0)\varphi(T)$ becomes small, since $\varphi(T > T_{dp}^r) \ll 1$. For the sake of clarity - there are two types of thermal motion of vortex lines in the presence of pinning centers: (i) Phonon-like, with small amplitude fluctuations affecting an individual pinning potential - *intravalley* fluctuations, thus smoothing the pinning potential and reducing $j_c(T)$ significantly near T_{dp}^r . (ii) The second kind of thermal motion is related to large *intervalley* thermal fluctuations, which cause jumping of vortices from one to another pinning center (valley). These are mainly responsible for the vortex-creep phenomena - which is not studied here. Here, we deal with type (i) thermal effects in the regime of the single-vortex pinning. Above and at T_{dp}^r the amplitude of the thermal fluctuations $\langle u^2 \rangle_{\text{th}}^{1/2}$ increases beyond the extent of the vortex core, $\langle u^2 \rangle_{\text{th}} > \xi^2$. In that case, the vortex experiences smaller averaged pinning potential. The calculation of T_{dp}^r is sophisticated and based either on: (i) the analogy of the vortex statistical physics with columnar defects and the quantum 2D-Bose gas placed in a random pinning potential, or (ii) on the statistical physics of vortices [19]. It turns out that for $r \gtrsim \sqrt{2}\xi_0$ the depinning temperature T_{dp}^r is approximately given by the self-consistent equation $T_{dp}^r \approx r \cdot \sqrt{\epsilon_p(T_{dp}^r)\epsilon_0(T_{dp}^r)}$, where $\epsilon_p(T) = \eta_{\text{col}} \cdot \Phi_0^2 / 32\pi^2 \lambda^2(T)$ and $\epsilon_0 = \Phi_0 / 16\pi^2 \lambda^2(T)$ [19].

III. TEMPERATURE BROADENING OF RESISTANCE IN THE MAGNETIC FIELD IN H_3S

In Refs. [10]-[13] it was claimed that in order to explain the temperature broadening of the resistance in magnetic field (*TBR*), $\delta t_c(h) \equiv (T_c - T_c(h))/T_c$, in HP-hydrides and in the framework of physics of soft superconductors, it is necessary to invoke an unphysically large critical current density $j_{c0} > 10^9 \text{ A/cm}^2$. In the case of the questionable CSH superconductor even much larger critical current is needed, i.e. $j_{c0} > 10^{11} \text{ A/cm}^2$ - where $\delta t_c(h)$ is field independent [7]. In the following it is argued, that

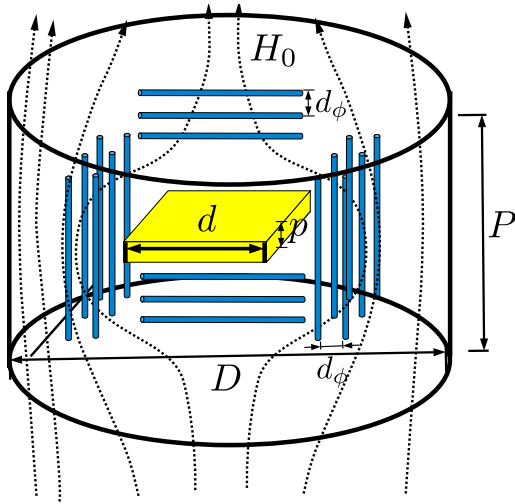


FIG. 2: Schematic view of the experiment of the magnetic flux trapping and penetration in the H_3S disk-like sample [1]: $D = 30\mu\text{m}; P = 5\mu\text{m}$ for the perpendicular geometry $\mathbf{H}_0 \perp D$. According to the SCPC-model, long columnar defects (*blue cylinders*) strongly pin and trap vortices making huge magnetization hysteresis and the critical current density $j_c \sim \delta M$. The non-superconducting ^{119}Sn film (*yellow* with $d = 20\mu\text{m}; p = 2.6\mu\text{m}$) is implemented in the experiment for the detection of the penetrated magnetic field [3]. Similar analyzes holds for the parallel geometry $\mathbf{H}_0 \parallel D$.

the reduction of $\delta t_c(h)$ in H_3S can be explained by invoking the SCPC model - which assumes that H_3S is a *hard type - II superconductor* with elongated intrinsic columnar pinning defects. The geometry of the experiment is shown in *Fig. 2*.

Let us briefly introduce the reader into the subject of *TBR* in H_3S , which is based on the Tinkham theory for *TBR* [22] and the SCPC model [1].

Namely, in all superconductors dissipationless current can flow in the vortex state with pinning defects. However, when the pinning energy is small, especially for T near T_c , vortices jump easily from one center to another under temperature fluctuations, thus giving rise to a vortex motion and dissipation of energy - called flux creep [23]. These jumps are activation-like and proportional to the escape probability (from the pinning center) $\exp(-U_p/T)$. Since for point defects $U_p^{\text{pd}} \sim \xi^3$, then this energy barrier is small in superconductors with small ξ , what is, for instance, the origin of a pronounced dissipation in HTSC-cuprates (with oxygen vacancies). In that sense, the long pinning defects with the energy $U_p \sim L_v \xi^2$ make this barrier much higher, thus suppressing the dissipation effects significantly. In magnetic fields much higher than the lower critical field, i.e. for $H_{c1} \ll H < H_{c2}$, one has $B \approx \mu_0 H$ and the vortex distance is given by $a \approx (\Phi_0/B)^{1/2} < \lambda$. In that case bundles of vortices, each with the surface $\sim a^2$, are pinned [24] with the pinning energy of the bundle $U_p \sim L_v a^2$. The Tinkham *TBR* theory [22] applied to such problems is based on the Ambegaokar and Halperin theory

for thermally activated phase motion in Josephson junctions [25]. As the result, it gives for the resistance of the superconductor (with small transport current) [22]

$$R/R_N \approx [I_0(\gamma/2)]^{-2}, \gamma = U_p/T, \quad (3)$$

where R_N is the resistance of the normal state at T_c and I_0 is the modified Bessel function.

In the SCPC model with *columnar pinning* centers with $L \approx L_v$ and near T_c one obtains for γ

$$\gamma^{\text{scpc}} = \beta_K \left(\frac{L_v}{\xi_0} \right) \frac{(1-t)^2}{h} (2\pi \xi_0^2 \frac{j_{c0} \Phi_0}{cT_c}), \quad (4)$$

where $h \approx H/H_{c2}(0), \delta t_c \equiv (1-t) \equiv 1 - T/T_c$ and $\beta_K \approx 1$. In the case of *point defects* one has for γ

$$\gamma^{\text{pd}} \approx \frac{(1-t)^{3/2}}{h} (2\pi \xi_0^2 \frac{j_{c0}^{\text{pd}} \Phi_0}{cT_c}). \quad (5)$$

Here, the critical current for weak pinning $j_{c0}^{\text{pd}} = \eta_{\text{pd}} \cdot j_{c0}$ is defined via the weak pinning energy $U_p^{\text{pd}} \approx \eta_{\text{pd}} H_c^2 \xi^3$ with $\eta_{\text{pd}} < 1$, while in the SCPC model one has $j_{c0} = \eta_{\text{col}} \cdot j_{c0}^{\text{max}}$ - see Eq. (1). The critical current density for weak pinning centers is usually of the order $j_{c0}^{\text{pd}} \sim 10^6$ A/cm². Note, that $\gamma^{\text{scpc}} \sim (1-t)^2/h$ for long columnar defects, while $\gamma^{\text{pd}} \sim (1-t)^{3/2}/h$ for point defects. The latter fact gives rise to the different temperature dependence of the irreversible line $H_{\text{irr}}(T)$ in HTSC (with oxygen vacancies as point defects) and H_3S - see more below. From these expressions it is seen, that the relative barrier in the case of long columnar pinning centers is larger by the factor $(L_v/\xi_0) \gg 1$, compared with the one for point-like randomly distributed defects - used in [10]-[13]. This means that j_{c0}^{pd} for point defects is replaced by much larger quantity $(L_v/\xi_0) \times j_{c0}$ in the SCPC-model - where one has $(L_v/\xi_0) \times j_{c0} \gg j_{c0}$.

Let us compare the prediction of the standard theory for weak pinning (with point-like defects) applied to H_3S - done in [10]-[13]. In the case when the resistance is measured at the 10 % level, i.e. $R/R_N = 0.1$, it gives for $I_0(\gamma/2) \approx 3.2$ and $\gamma \approx 5 (= \gamma^{\text{scpc}} = \gamma^{\text{pd}}$ in both cases. In the field $B \approx \mu_0 H \approx 1\text{T}$ and for $\mu_0 H_{c2}(0) \approx 100\text{T}$ one has $h \approx 0.01$. We assume also the following realistic parameters for the HP-hydrides: $\xi_0 \approx 20\text{\AA}$ and $T_c \sim 200\text{K}$, $\Phi_0 = 2 \times 10^{-7} \text{G} \times \text{cm}^2$. If one takes $j_{c0}^{\text{pd}} = \alpha j_{c0} \approx \alpha \times 10^7$ A/cm² with $\alpha \sim 0.1$, then by using Eq.(5) one obtains

$$\delta t_c^{\text{pd}} \equiv \frac{\delta T_c^{\text{pd}}(h = 0.01)}{T_c} \approx \frac{0.1}{\alpha}. \quad (6)$$

This is a too large value ($\delta t_c^{\text{pd}} > 0.1$) - see the red line in *Fig. 3*, compared to the experimental one $\delta t_c^{\text{exp}} \lesssim 10^{-2}$ [2]. Based on Eq.(5) one concludes that in order to explain the experimental value $\delta t_c^{\text{exp}}(h = 0.01) \lesssim 10^{-2}$ in H_3S in the framework of the weak pinning theory one needs a much larger (effective) critical current $j_{c0}^{\text{pd}} > 3 \cdot 10^8$

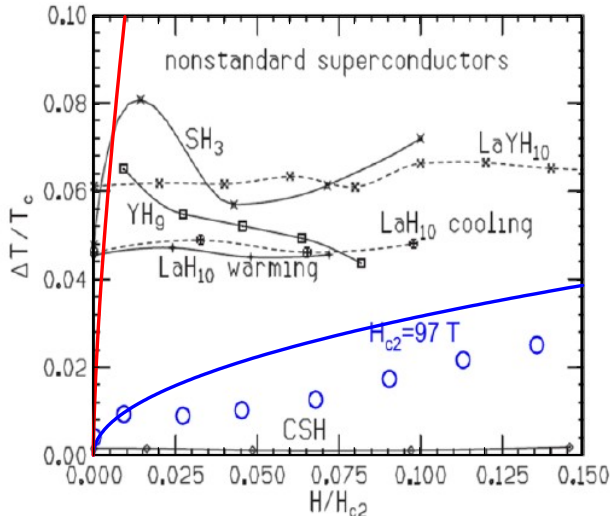


FIG. 3: Broadening of the superconducting transition (TBR) $\delta t_c(h) \equiv \Delta T/T_c$ under external magnetic fields in different superconducting HP-hydrides derived in Ref. [10] - points and solid lines and the experimental values for TBR in H_3S extracted in [2] - blue points. Blue line - the theoretical line predicted by the SCPC-model $\delta t_c^{scpc}(h) \sim h^{1/2}$ ($h = H/H_{c2}$, $H_{c2} \approx 100T$) for $j_{c0} \approx 10^7 A/cm^2$ and $L \approx 0.5\mu m$. The model is more suitable for low $h \leq 0.01$ - see text. Red line - the prediction of the standard model for TBR with weak-pinning $\delta t_c^{pd}(h) \sim h^{2/3}$ and for $j_{c0} \approx 10^7 A/cm^2$ is inadequate for H_3S .

A/cm^2 . However, the latter value is far beyond the range of the weak pinning theory.

However, the experimental value $\delta t_c^{exp} \lesssim 10^{-2}$ can be explained by the SCPC model with the long columnar pinning defects, where the $\delta t_c^{scpc}(h)$ depends on the large factor $(L/\xi_0) \times j_{c0}$, thus making $\delta t_c^{scpc}(h)$ small. In the case of H_3S where $\gamma_{00} = 2\pi\xi_0^2 \times j_{c0} \Phi_0 / cT_c$ and j_{c0} is in the range $j_{c0} > 10^7 A/cm^2$ (in CGS units $j_{c0} > 3 \times 10^{16}$ esu/cm²) and for $L_v \sim (0.5 - 1) \mu m$ one obtains

$$\delta t_c^{scpc}(h) \approx \left(\frac{5\xi_0 h}{L_v \gamma_{00}} \right)^{1/2} \lesssim 0.01. \quad (7)$$

The obtained result for TBR in Eq. (7) in the SCPC-model for $h \approx 0.01$ and $j_{c0} \sim 10^7 A/cm^2$ is in satisfactory agreement with the experimental values shown in Fig. 3 - the blue line. Since $\delta t_c^{scpc} \ll \delta t_c^{pd}$ this means that the SCPC model is able to describe TBR in the H_3S superconductor.

Note, that there is TBR also in the zero magnetic field ($H = 0$), i.e. there is an intrinsic TBR , $\delta T_0 \neq 0$, which should be taken into account in the analyzes of experiments. This was done in [2] and [10], where one has $\delta T_c(h) \approx \delta T_{tot}(h) - \delta T_{c0}$ and δT_{tot} is the total TBR . The extracted experimental results for $\delta t_c(h) (\equiv \delta T_c(h)/T_c)$

in H_3S are shown in Fig. 3 [2] - blue circles, for h within the range of $0 < h < 0.15$.

We stress again, that in order to explain the much smaller TBR , $\delta t_c(h)$, in H_3S (and in other HP-hydrides) than the standard Tinkham theory predicts for the weak pinning - see Eq.(5), the authors of [10]-[13] assume an unrealistically large critical current density $j^{pd} \sim (10^9 - 10^{11}) A/cm^2$. The latter value is much larger than the experimental one $j_{c0}^{exp} \gtrsim 10^7 A/cm^2$. The second possibility is to call into question the existence of superconductivity in HP-hydrides. This (second) possibility is accepted in [10]-[13]. However, in the proposed SCPC model j_{c0} in the formula for $\delta t_c(h)$ is in fact replaced by the much larger quantity $(L_v/\xi_0) \times j_{c0}$ - see Eq.(4), which for $(L_v/\xi_0) \sim 10^3$ gives realistic values for $j_{c0} \gtrsim 10^7 A/cm^2$. This analysis confirms our claim, that there is no reason to call into question the existence of the conventional superconductivity in H_3S .

IV. PENETRATION OF THE MAGNETIC FIELD IN H_3S

In order to confirm the existence of superconductivity in a sample, two kinds of experiments in an external magnetic field are necessary: (i) At $T > T_c$ the sample is placed in a magnetic field $H < H_{c1}$ (or H_c in type-I superconductors) and then cooled below T_c - the *FC* (field cooled) experiment. If the magnetic field is expelled from the sample the *Meissner effect* is realized. Its existence means a definitive proof for superconductivity in the sample; (ii) In the *zero field cooled (ZFC)* experiment the sample is first cooled to $T < T_c$ at zero external field ($H = 0$) and then is the field $H < H_{c1}$ applied. In this case, the magnetic field is excluded from the sample - the so called *diamagnetic shielding mode*. The latter effect is in fact due to the well known Lenz law in electrodynamics. In the Meissner state of type-I superconductors currents in a bulk sample decay exponentially from the sample surface and the average current over the bulk sample is zero. In an ideal type-II superconductor with regular vortex lattice the average circulating current (around the vortices) is also zero. A net average (transport) current can exist only due to distortions of the vortex lattice in the presence of pinning defects. As a result, the transport current can flow in bulk type-II superconductors, $j(r) \neq 0$, and the field can penetrate into the sample at much larger distance than the penetration depth λ . If the pinning is strong (and the critical current large) such superconductors are called hard superconductors.

In Section III the theoretical (in the SCPC-model) and experimental results for TBR suggest, that H_3S (and other HP-hydrides) is a hard type-II superconductor, with large Ginzburg-Landau parameter $\kappa (= \lambda/\xi) = (50 - 100)$ and high (low-temperature) critical current density $j_{c0} \gtrsim 10^7 A/cm^2$. Next questions related to H_3S are: (i) What is the prediction of the SCPC model for the penetration of magnetic field (*PMF*) into a supercon-

ducting sample; (ii) How big is the magnetic hysteresis observed in H_3S [3]? For simplicity, these questions are analyzed quantitatively in the framework of the Bean critical state model - first for a long cylinder and then for a disk with small thickness $P(\ll D)$. Afterwards, the theory is compared with the experiment in H_3S [3]. In the following, the results are presented either in the CGS or in SI units - according to the existing magnetic measurements. B^0 , B_0 and B_{ext} are equivalent labeling for the applied magnetic field (induction). Some problems related to the *FC* Meissner effect are discussed at the end of this Section.

A. Experimental results for the ZFC field penetration in H_3S

The *ZFC* penetration depth is studied experimentally in H_3S by the novel NRS technique [3] - the geometry of the ZFC experiment is shown in *Fig. 2*. The experiment measures the time evolution of the scattered radiation re-emitted by the ^{119}Sn film - *Fig. 3* in Ref. [3]. In this ZFC experiment a non-superconducting thin ^{119}Sn film is placed inside the H_3S disk-sample (see *Fig. 2* - yellow color) being used as a sensor of the magnetic field. The internal magnetic field on the ^{119}Sn sensor is monitored by the nuclear resonance scattering of synchrotron radiation. When the magnetic field penetrates in the ^{119}Sn non-superconducting film, the experimental curve for the radiation intensity as a function of time shows *quantum beats*, due to the interference of the split ^{119}Sn nuclear levels by the magnetic field. These beats are indeed observed in the field $B^0 = 0.68$ T at $T > T_c$ - when the sample is non-superconducting and the perpendicular magnetic field penetrates completely into the ^{119}Sn film - *Fig. 3* in Ref. [3]. Note, that since H_3S is a type II superconductor one expects that if the sample is free of pinning centers, then for $B^0 \gg \mu_0 H_{c1} = (18 - 60)$ mT the magnetic field should enter into the whole sample in the form of (almost) homogeneously distributed vortices - thus showing quantum beats in the ^{119}Sn film. However, in the *perpendicular geometry* of the experiment ($\mathbf{H} \perp D$ in *Fig. 2*) at low temperatures and in the field $B^0 = 0.68$ T [3] the vortices do not show up in the center of the ^{119}Sn film up to some temperature, i.e. there are no quantum beats - *Fig. 3* in [3]. This means that the vortices are strongly pinned in the region outside of the ^{119}Sn film. Strong pinning of vortices in a superconductor implies, that the magnetization of the sample is strongly hysteretic, as revealed experimentally in H_3S - see [2],[4],[14].

Two geometries were studied in [3]: (A) The *perpendicular geometry* - where the field is perpendicular to the disk surface ($\mathbf{H} \perp D$ in *Fig. 2*); (B) The *parallel geometry* - the field is parallel to the disk surface ($\mathbf{H} \parallel D$). As it is seen in *Fig. 4A* the average field inside the ^{119}Sn sensor in the perpendicular geometry is approximately zero for $T < 80$ K and reaches the value $B_{\text{ext}} = 0.68$ T

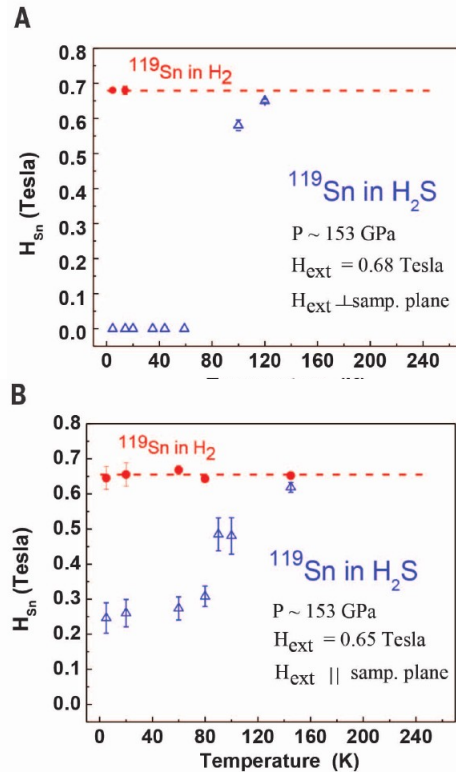


FIG. 4: The experimental temperature dependence of the magnetic field on the sensor ^{119}Sn film (placed) inside H_3S (see *Fig. 2*) at 153 GPa shown by blue triangles. The external field at the reference non-superconducting sample ^{119}Sn in H_2 at 150 GPa is shown by red dots - see [3]. (A) and (B) are measurements in the perpendicular ($H_{\text{ext}}^\perp \perp D$) and parallel ($H_{\text{ext}}^\parallel \parallel D$) geometry of the external magnetic field, respectively. Dashed lines are guides to the eye. Taken from [3].

at around $T \approx 120$ K. In the parallel geometry the field inside the ^{119}Sn film is finite for $T > 0$ (but smaller than $B_{\text{ext}} = 0.68$ T) starting to increase at $T > 80$ K saturating to $B_{\text{ext}} = 0.68$ T at $T \gtrsim 140$ K - *Fig. 4B*. In the next Subsection these experimental results are explained by the theory which is based on the Bean critical state model and the SCPC model with high critical current density $j_{c0} \geq 10^7 \text{ A/cm}^2$.

B. Penetration of the magnetic field in a long cylinder with pinning centers

In Section III it is argued, that the experimental results on the thermal broadening of resistance (*TBR*) in magnetic field in H_3S , $\delta t_c^{\text{exp}}(h)$, give much smaller value than those predicted by the Tinkham theory for standard superconductors with weak pinning, i. e. $\delta t_c^{\text{exp}}(h) \ll \delta t_c^{\text{pd}}(h)$. However, the SCPC model with

the columnar pinning centers and large critical currents $j_c(0) > 10^7 \text{ A/cm}^2$ explains this property, i. e. $\delta t_c^{\text{scpc}}(h) \approx \delta t_c^{\text{exp}}(h)$. Note, that the large value of $j_c(0)$ inevitably causes large magnetization hysteresis, which is seen experimentally in H_3S [2],[4],[14]. The critical current density $j_c(0)$ is a measure of the strength of pinning forces. Below, it is shown that the large value of $j_c(0)$ is compatible with experiments for the penetration of the magnetic field into thin H_3S film [3]. To maximally simplify the problem a long cylinder placed in the external field $B_0 = \mu_0 H_0$ is first considered (in absence of external transport currents), thus escaping demagnetization effects. This case is also used in studying the field penetration in the parallel geometry of H_3S , i.e. when $B_0 \parallel D$.

In an homogeneous system in thermodynamic equilibrium, in an ideal type II superconductor (without pinning centers), vortices are homogeneously distributed over the bulk sample. In that case the macroscopically averaged (over the sample) local magnetic induction is constant, i.e. $\bar{\mathbf{B}}_{\text{eq}}(\mathbf{r}) = \text{const}$ and the macroscopic local magnetization current density (averaged over the vortex unit cell) is zero, i.e. $\mu_0 \bar{\mathbf{j}}_{\text{eq}}(\mathbf{r}) = \text{rot} \bar{\mathbf{B}}_{\text{eq}} = 0$, as well as the Lorentz force per unit volume of the vortex lattice $\mathbf{f}^{\text{eq}}_L = \bar{\mathbf{j}}_{\text{eq}} \times \bar{\mathbf{B}}_{\text{eq}} = 0$. However, in the presence of pinning centers $\bar{\mathbf{B}}(\mathbf{r})$ is *inhomogeneous* and $\bar{\mathbf{j}}(\mathbf{r}) \neq 0$, thus producing finite Lorentz force (per unit volume) on vortices $\mathbf{f}_L = \bar{\mathbf{j}} \times \bar{\mathbf{B}} \neq 0$. When the vortices are pinned there is a pinning force (per unit volume) \mathbf{f}_p which counteracts the Lorentz force. In the static case the vortices are not moving and the condition $\mathbf{f}_L = -\mathbf{f}_p$ is fulfilled everywhere in the sample. So, by increasing the applied field the vortices are so rearranged that locally the maximal critical current $\mu_0 \bar{\mathbf{j}}_c(B) = \text{rot} \bar{\mathbf{B}}$ is achieved.

The simplest, but very useful, model for the critical state is the *Bean critical state model* [26], which assumes that j_c is independent on B . In the case of a *long cylinder* $L \gg R$ (no demagnetization effects) one has $d\bar{B}/dr = \pm \mu_0 \bar{j}_c$ and $\bar{B}(r)$ is given by

$$B(r, B_0) = B_0 - B^*(T) \left(1 - \frac{r}{R}\right). \quad (8)$$

It is seen from Eq.(8) that for an applied field $0 \leq B_0 < B^*$ the field $B(r)$ penetrates up to the point $r_{B_0} = (1 - B_0/B^*)R$, where $B(r_{B_0}, B_0) = 0$. At $B_0 = B^*$ the field reaches the center of the cylinder, i.e. at $r_{B^*} = 0$ one has $B(r_{B^*} = 0, B^*) = 0$ - see Fig. 5. In the experiment [3] - schematically given in Fig. 2, one has $D = 30 \mu\text{m}$ and by assuming that $L \gg D$ one has $1.8 \text{ T} < B^*(j_{c0}) < 18 \text{ T}$. This range for $B^*(j_{c0})$ is due to j_{c0} in the range $j_{c0} \approx (10^7 - 10^8) \text{ A/cm}^2$.

However, the applied field in the experiment by Troyan et al. [3] was fixed to $B_0 = 0.68 \text{ T}$, i.e. $B_0 < B^*(T \ll T_c)$. This means that at very low temperature ($T \ll T_c$) the field does not penetrate into the center of the non-superconducting ^{119}Sn film, if the sample would be a long cylinder with $L(=P) \gg D$. Note, that the magnetic field reaches the front of the ^{119}S

film at $r_{B_0^S} = 10 \mu\text{m}$, i.e. for $B_0^S = (1/3)B^*$ where $B_0^S \approx (0.6 - 6) \text{ T}$, for $j_{c0} \approx (10^7 - 10^8) \text{ A/cm}^2$. Therefore, in the case of a long cylinder with $L(=P) \gg D$ at low T with $j_{c0} \approx 1.5 \times 10^7 \text{ A/cm}^2$ placed in the external field $B_0 = 0.68 \text{ T}$, the field would not be able to penetrate neither the front of the ^{119}S film (where $r_{B_0^S} = 10 \mu\text{m}$) nor the center ($r_{B^*} = 0$) of the sample, since $B_0 < B_0^S < B^*$.

We stress again, that the experiment in Ref. [3] was performed on a finite-size sample in two geometries: (A) the *perpendicular* geometry when the magnetic field is perpendicular to the thin cylinder, i.e. $B_0 \perp D$ - see Fig. 2, and (B) in the *parallel geometry* when the field is parallel to the diameter D of the sample, i.e. to the surface of the thin disk with $P \ll D$. In the next Subsection it is shown, that in the case (A) finite size effects are very important, while in the case (B) they are less pronounced and the problem can be, in the first approximation, treated as a long cylinder, since $P \ll D$.

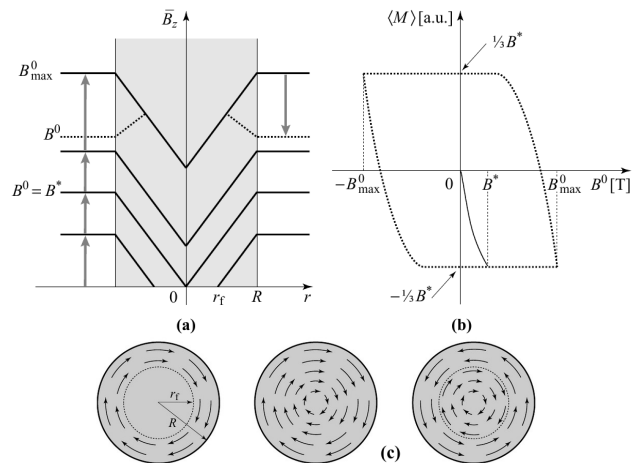


FIG. 5: The Bean critical state model for a long cylinder with radius $R \ll L$: (a) distribution of local averaged field $\bar{B}(r)$ in the external field B^0 parallel to the surface of the cylinder - *up* arrow for increased B^0 from 0 to B_{max}^0 and *down* arrow for decreased B^0 from B_{max}^0 to B^0 . For $B^0 = B^*$ the field penetrates to the center of the sample, where $\bar{B}(0) = 0$; (b) the hysteresis loop for the magnetization $M_{\text{ir}} = \langle \bar{M} \rangle$ (averaged over the cylinder) - the virgin (initial) line in *bold*; (c) distribution of the current density in the superconducting cylinder in an axial field: *left* - in the increasing field from $B^0 = 0$ to $B^0 < B^*$ the screening current flows between r_f and R where $\bar{B}(r_f) = 0$; *middle* - for $B^0 > B^*$ it flows in the whole sample; *right* - in decreasing field from B_{max}^0 to B^0 the current is inverted in the external sheath. From [27].

C. Theory for the penetration of the magnetic field in H_3S - perpendicular geometry

In the perpendicular geometry $B_0(= \mu_0 H_0) \perp D$ of the thin disk with $L \ll R$ (i.e. $P \ll D$ in the experiment of Ref. [3] - see Fig. 2) there is a geometric barrier when the sample shape (due to geometric spikes) is different from

an ellipsoid. It turns out, that in that case the magnetic field penetrates into the sample in an inhomogeneous way [28]. The theory [28] predicts that in the perpendicular geometry the flux is penetrated up the center in the external field $B_{0\perp} = B_{p\perp}$ with

$$B_{p\perp}(T) = B^*(T) \frac{P}{D} \ln \left[\frac{D}{P} + \sqrt{\left(1 + \frac{D^2}{P^2}\right)} \right], \quad (9)$$

where $B^*(T) = \mu_0 j_c(T) D/2$. In order to explain the temperature dependence of the field in the ^{119}Sn sensor [3] - see *Fig. 4A*, we define an *effective field* on the ^{119}Sn sensor

$$B_{Sn}^\perp(T) \equiv B_0 - B_{p\perp}(T). \quad (10)$$

(Here, T is the absolute temperature.) By definition, for $B_0 \leq B_{p\perp}(T)$ one has $B_{Sn}^\perp = 0$, i.e. the field does not reach the center of the sample. When, $T \ll T_c$, $j_{c0} \approx (1.4 - 1.5) \times 10^7 \text{ A/cm}^2$ - see *Fig. 6A*, and $(P/D) \approx 1/6$ - see *Fig. 2*, one has $B_{p\perp} \approx 1\text{T}$ which gives that

$$B_0 (= 0.68\text{T}) < B_{p\perp}. \quad (11)$$

This means, that the external field is not strong enough to push the pinned vortices to the center of the sample. However, in order to study the temperature dependence of $B_{Sn}^\perp(T)$ it is necessary to know the temperature dependence of the current density $j_c(T)$. In that respect, one should take into account two effects: (a) The (mean field) temperature dependence of $\lambda(T)$ and $\xi(T)$ since $j_c(T) \sim \lambda^{-2}(T)\xi^{-1}(T)$. In the temperature range $0 < T \leq T_c/2$ we mimic $\lambda^{-2}(T)\xi^{-1}(T) \sim (1 - T^2/T_c^2)^3$; (b) The temperature fluctuations cause depinning effects (see **II.C**) which decrease $j_c(T)$ additionally - even bringing it almost to zero at some T_{dp}^r - see *Fig. 1* and *Fig. 6*. For the sake of simplicity, $\varphi(T)$ is described approximately by the linear function $\varphi(T) \approx (T_{dp}^r - T)/(T_{dp}^r - T_{kink})$ for $T \geq T_{kink}$. As the result, one obtains $j_c(T) = j_{c0} \cdot \varphi(T)(1 - T^2/T_c^2)^3$. The fit of the experimental curve in *Fig. 6A* is obtained for $T_{kink,\perp} \approx 101\text{K}$ and $T_{dp,\perp}^r \approx 122\text{K}$ which gives the theoretical curve for $B_{Sn}^\perp(T)$ shown in *Fig. 6A*.

It is important to point out, that the theoretical curve $B_{Sn}^\perp(T)$ (in *Fig. 6A*) fits the experimental results (in *Fig. 4A*) if the current density is high, i. e. $j_{c0} \approx 1.4 \times 10^7 \text{ A/cm}^2$. This value for j_{c0} is compatible with the one obtained from the *TBR* measurements in H_3S , where $j_{c0} \gtrsim 10^7 \text{ A/cm}^2$. Both findings confirm the assumption of the SCPC model, that the intrinsic defects in H_3S are approximately elongated columns, which pin vortices strongly, thus giving high critical current densities in this material.

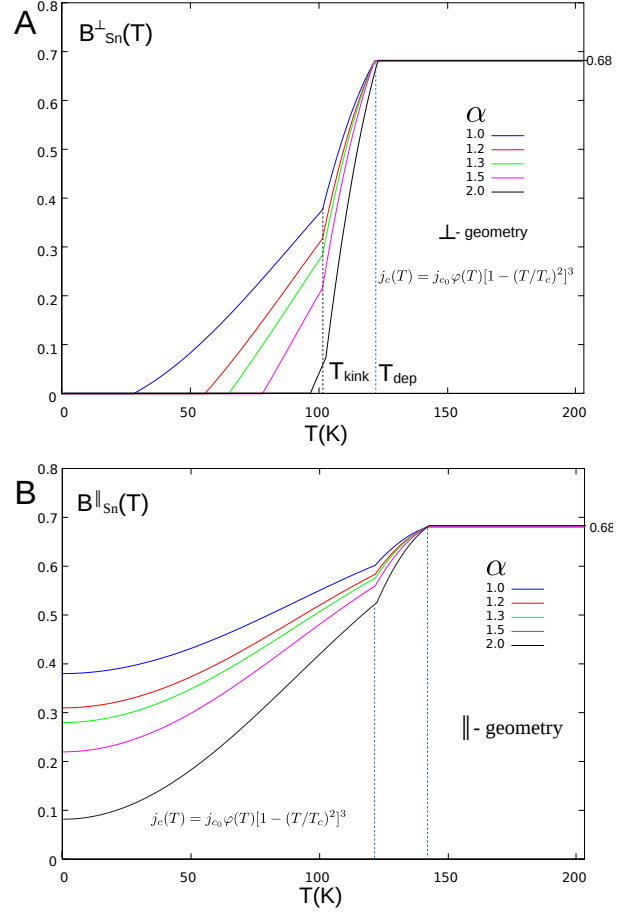


FIG. 6: The temperature dependence of the effective magnetic field $B_{Sn}(T)$ in the ^{119}Sn sensor in the combined Bean model and the SCPC-model. For T_{kink} and $T_{dep}(\equiv T_{dp}^r)$ see text. **A** - $B_{Sn}^\perp(T)$ in the perpendicular geometry; **B** - $B_{Sn}^\parallel(T)$ in the parallel geometry. The various curves are for different current densities $j_{c0} = \alpha \times 10^7 \text{ A/cm}^2$; $\alpha = 1, 1.2, 1.3, 1.5, 2.0$

D. Theory for the penetration of the magnetic field in H_3S - parallel geometry

Similarly, when the field is parallel to the thin disk, i.e. $B^\parallel(T) \parallel D$ - see *Fig. 1*, the effective field on the ^{119}Sn sensor is given by

$$B_{Sn}^\parallel(T) \equiv B_0 - B_{p\parallel}(T). \quad (12)$$

In this geometry and with $P \ll D$ - see *Fig. 2*, the system can be approximated by a long cylinder with $R \approx P/2$ and $L \approx D$. In that case the formula Eq.(8) holds approximately, which gives $B_{p\parallel}(T) \approx \mu_0 j_c(T) P/2$. For assumed value $j_{c0} \approx 1.4 \times 10^7 \text{ A/cm}^2$ one obtains $B_{p\parallel}(T \ll T_c) \approx 0.45 \text{ T}$, which is smaller than the applied field $B_0 = 0,68 \text{ T}$, i.e.

$$B_{p\parallel}(T \ll T_c) < B_0 (= 0,68\text{T}) \quad (13)$$

This means, that $B_{\text{Sn}}^{\parallel}(T \ll T_c) > 0$ and the external field B_0 is large enough to push vortices into the center of the ^{119}Sn film - see *Fig. 6B*, which is in agreement with the experimental result in *Fig. 4B*. The fit of $\varphi(T)$ (note, that $j_c(T) \sim \varphi(T)$) is analogous to the perpendicular case but with slightly different parameters $T_{\text{kin},\parallel} \approx 122\text{K}$ and $T_{\text{dp},\parallel}^r \approx 142\text{K}$. Note, that there is a qualitative difference between $B_{\text{Sn}}^{\perp}(T)$ and $B_{\text{Sn}}^{\parallel}(T)$, since $B_{\text{Sn}}^{\perp}(T)$ is zero up to some finite temperature - see *Fig. 4* and *Fig. 6*, and $B_{\text{Sn}}^{\parallel}(T)$ is finite even at $T = 0\text{K}$. This is due to different sample dimensions, i.e. that $P \ll D$ - see *Fig. 2*. These results are in a qualitative and semi-quantitative agreement with the experimental results in [3].

It is necessary to point out following items: (a) It is seen in *Fig. 5*, that in the Bean critical state model the irreversible magnetization for a long cylinder in fields $B_0 > B^*$ is constant (field independent). Since the measurements of the magnetic moment of the H_3S sample in [3] are given in the CGS unit emu we use it also here. After averaging of $\bar{M} = (\bar{B} - H)/4\pi$ over the sample one has $\bar{M}_{\text{ir}}(\text{emu}/\text{cm}^3) \approx (R/30)j_c(\text{A}/\text{cm}^2)$ and the total magnetic moment $\mu_{\text{ir}} = \bar{M}_{\text{ir}} \cdot V_s$. Note, that $\bar{M}_{\text{ir}} = (\bar{M}_+ - \bar{M}_-)/2 = \bar{M}_-$ since in the Bean model $\bar{M}_+ = -\bar{M}_-$ holds for $B_0 > B^*$. For the volume of the disk $V_s \approx 0.8 \times P \cdot D^2$ one obtains the trapped magnetic moment in the sample to be of the order $\mu \approx (0.3 - 2) \times 10^{-5}$ emu for $B_0 > B_{p\perp}$ and for $j_{c0} \approx (1.4 - 10) \times 10^7 \text{A}/\text{cm}^2$. The calculated *trapped* magnetic moment in the H_3S sample of Ref.[3] is far beyond the SQUID sensitivity threshold - which is $\sim 10^{-8}$ emu [3]. This means that the measurements of the trapped magnetic flux of vortices (but without the extrinsic moments) are realizable. (b) In order to explain the field penetration in the H_3S sample of Ref. [3] it comes out that the perpendicular ($\mathbf{H} \perp D$) critical current density j_{c0}^{\perp} must be approximately equal to the parallel ($\mathbf{H} \parallel D$) one j_{c0}^{\parallel} , i. e. $j_{c0}^{\perp} \approx j_{c0}^{\parallel}$. This means, that in the H_3S sample of Ref. [3] the columnar defects are oriented along both directions, the parallel and perpendicular one, in a similar way - schematically shown in *Fig. 2*. Having in mind the cubic-like structure of H_3S this kind of pinning isotropy is an acceptable assumption; (c) In order to explain the *TBR* and *PMF* measurements in thin H_3S samples in the SCPC model, it comes out that the bulk H_3S sample is a high- κ type II superconductor with the parameters: $\xi_0 \approx (15 - 20) \text{\AA}$, $\lambda_0 \approx (1 - 2) \times 10^3 \text{\AA}$; $\kappa \approx (50 - 100)$, $\mu_0 H_{c1} \approx (18 - 60) \text{mT}$, $\mu_0 H_{c0} \approx (0.6 - 1.1) \text{T}$, $\mu_0 H_{c2} \approx (80 - 140) \text{T}$. These values are very different from those obtained in [2], [14], where $\xi_0 \sim 20 \text{\AA}$, $\lambda_0 \sim (1.3 - 2) \times 10^2 \text{\AA}$; $\kappa \sim 7 - 10$, $\mu_0 H_{c0} \sim 6 \text{T}$, $\mu_0 H_{c1} \sim 1 \text{T}$, $\mu_0 H_{c2} \approx (80 - 140) \text{T}$. The values of the parameters predicted in the SCPC model are compatible with those obtained in the magnetic measurements and also with the microscopic theory - see the discussion below.

To this point, Hirsch and Marsiglio have recently realized [29], that their previous interpretation [10]-[11] of the Troyan's measurements in H_3S [3] in terms of pinning-free

superconductors with unphysically high $j_{c0} \sim 10^{11} \text{A}/\text{cm}^2$ may be inadequate. Namely, due to the pronounced magnetization hysteresis in [4] they speculated the presence of pinning forces in H_3S - with the critical current density $j_{c0} \sim 10^7 \text{A}/\text{cm}^2$. However, they did not realize that the *TBR* and *PMF* effects in H_3S are due to the strong pinning by the elongated (columnar) defects - as the SCPC model predicts [1].

To conclude this Section - the magnetic measurements of the penetration of the magnetic field $B_0 = 0.68 \text{T}$ in the H_3S sample [3] can be naturally explained in the framework of the SCPC model and the Bean critical state model. This approach also explains naturally the high critical current density in the H_3S samples, which is of the order $j_{c0} \approx (1.4 - 1.5) \times 10^7 \text{A}/\text{cm}^2$. Thereby, the finite-size effects in the thin H_3S disk of Ref. [3] are taken into account. This analyzes tells us, that there is no need to call into question the existence of superconductivity in H_3S (and in other HP-hydrides), as it is claimed in [10]-[13].

E. Meissner effect in H_3S

The Meissner effect is an important hallmark of the superconducting state. It is realized in the so called FC (*field cooled*) *experiment*, when the sample (ideally without pinning defects) is in the normal state ($T > T_c$) and placed in a magnetic field $H_0 < H_{c1}$ (for type-II superconductors). The latter penetrates into the normal metallic sample fully, i. e. one has $B \approx \mu_0 H_0$. However, if the sample is then cooled down into the superconducting state ($T < T_c$) the magnetic field will be *expelled* from the bulk sample, i. e. one has $\bar{B} = 0$ in an ideal non-magnetic superconductor. The Meissner effect should not be confused with the ZFC (zero - field cooled) *experiment*, where a nonmagnetic bulk metallic sample is first cooled into the superconducting state at $T < T_c$ in the zero field ($H = 0$) and thereafter magnetic field $H < H_{c1}$ is turned on. As a result, the magnetic field (induction) is *excluded* from the bulk sample, i.e. $B = \mu H = 0$ with $\mu = \mu_0(1 + \chi) = 0$. The ZFC phenomenon is also called *diamagnetic shielding*. However, the ZFC effect would also be realized in a *perfect metal* (with $\varrho = 0$) - if it existed in nature, where it is due to the classical Lenz law of the electrodynamics. From this analyzes comes out, that the magnetic susceptibility of an ideal bulk superconductor is diamagnetic $\chi = -1$ in the SI system ($4\pi\chi = -1$ in the CGS) in both types of experiments. Note, that when the FC experiment is done in a perfect metal, the magnetic field is not expelled from the sample at $T < T_c$, i.e. the magnetic flux stays frozen in the sample with the same value as in the normal state, i.e. $B \approx \mu_0 H_0$. So, for a definite proof of the Meissner effect in superconductors one should perform the FC experiment.

In that respect, several inconsistent experimental and theoretical results related to the magnetization measure-

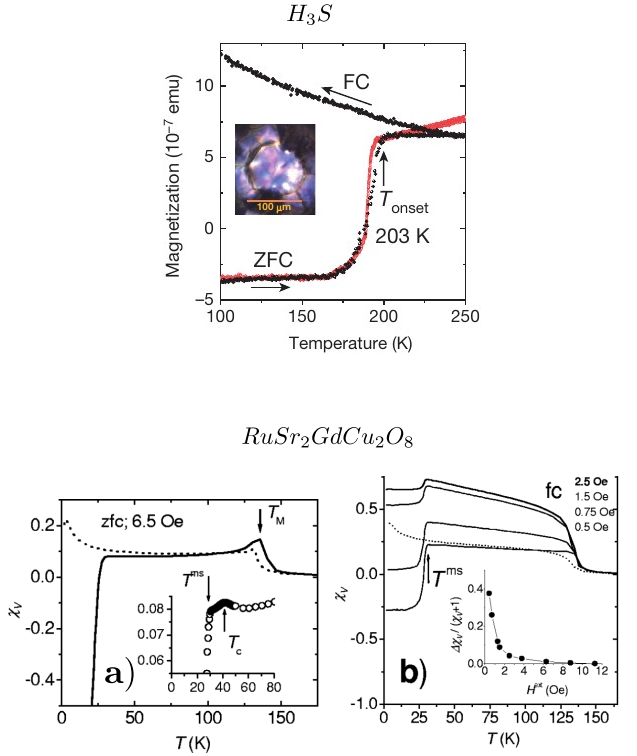


FIG. 7: *Up* - The FC and ZFC magnetization (M) in H_3S - from [2],[4]. *Down* - the volume susceptibility χ_V of the weak ferromagnetic superconductor $RuSr_2GdCu_2O_8$; **a**) - ZFC (zfc) measurements of χ_V at $H^{ex} = 6.5$ Oe; dotted line is χ_V in the non-superconducting state. $T_M \approx 137$ K is the magnetic critical temperature; $T^{ms} \approx 30$ K is the transition temperature to the spontaneous vortex state (SVS) which exists at $T^{ms} < T < T_c$. Inset: enlarged scale of χ_V around the superconducting transition $T_c \approx 45$ K; **b**) FC measurements of χ_V for external fields $H^{ex} \approx (0.5 - 2.5)$ Oe. Inset: The volume fraction of the Meissner state $f \approx 40\%$ at $H^{ex} = 0, 5$ Oe - from [15].

ments in H_3S (and LaH_{10}) were published (in the period 2015-2022) in [2],[4],[14]. These results are strongly criticized in [10]-[13]. We shall not elaborate this criticism in details, but enumerate few, in our opinion, main points by Hirsch and Marsiglio [10]-[13]. These are: (1) The Meissner effect is not observed experimentally in H_3S (and other HP-hydrides) [2],[4],[14]). Namely, in the FC measurements only some parasitic paramagnetic susceptibility is observed, i. e. $\chi_{FC}(T < T_c) > 0$, and there are no signs of the flux expulsion. However, in the ZFC experiment there is a clear diamagnetic shielding (at $T < T_c$) but existing on the background of the parasitic paramagnetic signal. Most probably, the origin of this paramagnetic signal is not intrinsic, since there is no reliable reason for strong paramagnetic effects in H_3S . To this point, there is also a pronounced para-

magnetic contribution in the FC measurements in the HTSC superconductor $RuSr_2GdCu_2O_8$ - with $T_c \approx 45$ K, where a weak ferromagnetism appears below $T_M \approx 137$ K [15]. At $T \geq T^{ms} \approx 30$ K a spontaneous vortex state (SVS) appears, where $H_{c1}(T) < M$ and M is the spontaneous magnetization. In *Fig. 7* it is seen, that in the FC measurements χ_v is paramagnetic, even for $T < T_c$, i. e. $\chi_V(T) > 0$. At $T^{ms} \approx 30$ K the susceptibility χ_V decreases suddenly and the sample is in the bulk Meissner state at $T < T^{ms}$ with the volume fraction $f = |(\chi_V(0) - \chi_V(T^{ms})) / (1 + \chi_V(T^{ms}))| \approx 40\%$ at $H^{ex} = 0, 5$ Oe - see Inset in *Fig. 7b*. This tells us that pinning centers are present in the $RuSr_2GdCu_2O_8$ sample.

Having in mind this analyzes, one expects that in the FC measurements in H_3S a sudden decrease of χ_V should be realized below T_c . However, so far, no such results have been published with clearly realized Meissner effect in HP-hydrides. The paramagnetic signal in the H_3S sample is most probable due to some extrinsic properties of the diamond anvil cell (or of the rest of the sulfur atoms, since H_2S is decomposed into H_3S and S) and this fact deserves further studies. (2) Additional critical remarks, given in [10]-[13], are related to some controversial findings in [14], that in the H_3S (and LaH_{10}) sample the critical fields $H_{c1}(0)$ and $H_c(0)$ are too large, while the penetration depth λ_0 is too small. If this is true, the large value of the critical field $\mu_0 H_{c1}(0)$ in [14] would give very high critical current density in H_3S (and LaH_{10}), i. e. $j_{c0} \sim 10^{10}$ A/cm². This is much higher value than the depairing current density $j_{dep} \simeq 5 \times 10^8$ A/cm², what is in fact impossible. The large value for $H_c(0)$ (in Ref. [14]) is incompatible with the microscopic theory of superconductivity, which relates the condensation energy to $H_c(0)$ by $(N(E_F)\Delta^2) = H_c^2(0)/8\pi$. Here, $N(E_F)$ is the density of states (per unit volume) at the Fermi surface. For $2\Delta \approx 3,5T_c$ and $\mu_0 H_c(0) \sim 10$ T (in [14]) one obtains that $N(E_F) \approx 30 \times N^{DFT}(E)$, while the density functional theory gives $N^{DFT}(E_F) \approx 0,2$ states/spin \times eV \times (\AA)³ [10]-[13]. Therefore, this highly overestimated value for the density of states, which are extracted from the magnetic measurements in H_3S [2],[4],[14], is an highly unacceptable value.

Let us discuss the origin of these too large values for the bulk critical fields $\mu_0 H_{c1}(\sim 1$ T) and $\mu_0 H_{c0}(\sim 10$ T) obtained in [14]. The latter result is based on an inadequate experimental definition of H_{c1} . Namely, it is determined from the onset field $\mu_0 H_p(0)(\sim 0.1$ T) of the deviation of $M(H)$ from the linear dependence by assuming that $H_{c1} = H_p(0)/(1 - N)$. In the measurements in Ref. [14] the demagnetization factor is $N \approx 0.96$, what gives too large value for $\mu_0 H_{c1}(T = 0) \approx 2$ T. That this procedure is not well defined, i. e. $H_p(0)$ is not related to H_{c1} , can be seen in *Fig. 5b* where $M(H)$ curve in the Bean critical state model, where the saturation field $H^*(P, D) \gg H_{c1}(0)$. In the perpendicular geometry of the experiment [3] one has $P = 5 \mu m$ and $D = 30 \mu m$, $N \sim 0.7$ and according to *Eq. (9)* one has $\mu_0 H_{p,\perp}(0) \approx 1$ T what is much larger than the real $H_{c1}(T = 0)$. If we

would apply the same procedure for obtaining H_{c1} in the H_3S sample, as it was done in Ref. [14], we would obtain also an unrealistic value $\mu_0 H_{c1}(T = 0) \approx 3$ T, instead of the realistic one $\mu_0 H_{c1}(0) \approx (18 - 60)$ mT.

V. SUMMARY AND DISCUSSION

Recently, the authors of Refs. [10]-[13] raised important questions on the reliability of magnetic measurements in high-pressure hydrides (HP-hydrides). Their skepticism goes so far, that they tend to conclude that superconductivity does not actually exist in HP-hydrides [10]-[13]. This attitude is mostly related to the FC magnetic measurements, which are until now unable to prove unambiguously the existence of the Meissner effect in small samples of H_3S . On the other side, some ZFC measurements, in small samples of H_3S , are experimentally more reliable, because these are not related to the flux trapping effects. There are also difficulties to explain some experimental results of magnetic measurements in H_3S - done in [2],[4],[14], if they are treated by the standard theory of superconductivity with weak pinning of vortices. The latter approach is mainly accepted in [10]-[13], thus reducing the possibility for explaining experiments in H_3S , such as: (i) TBR - the temperature broadening of resistance in magnetic field, and (ii) PMF - the penetration of the magnetic field into the center of the sample.

In order to explain these two kinds of experiments - which can not be explained by the weak pinning theory, Ref. [1] introduces the SCPC model - which holds for superconductors with strong and elongated pinning defects. Moreover, even the quantitative explanation of these two phenomena (in H_3S) is possible by assuming that the pinning centers are in the form of long columnar defects, which are “isotropically” distributed over the sample, i. e. with the same values of the critical current densities flowing perpendicular and parallel to the sample surface. In the framework of the SCPC model it is possible to explain these two kind of experiments. In the following we summarize the obtained results: **1.** The large reduction of TBR, $\delta t_c^{scpc}(h)$, is due to the long columnar defects $L \approx L_{v(ortex)} \gg \xi_0$ with the radius $r \sim \xi_0$. In such a case, both the core and the electromagnetic pinning are operative. These cause high densities of the critical current (at $T \ll T_c$) - of the order $j_{c0} = (10^7 - 10^8)$ A/cm². The SCPC model predicts, that in H_3S the temperature width of TBR is governed by the small parameter $C = \xi_0/L_{c01}$, i. e. $\delta t_c^{scpc}(h) \sim C^{1/2} h^{1/2}$ with $C \sim 10^{-3}$ and $h = H/H_{c2}$. This gives $\delta t_c^{scpc}(h) \lesssim 0.01$ for $h \lesssim 0.01$ and $L \sim 1$ μ m, which is in satisfactory agreement with experimental results in H_3S [2], as shown in Fig. 3. It is also seen that the SCPC model fits the experimental results much better than the model with weak pinning by small defects. The SCPC model also predicts, that the magnetic irreversible field is governed by C^{-1} , i. e. $H_{irr} \sim (1 - t)^2 L/\xi_0$. The irreversibility line is not only significantly increased compared to HTSC-cuprates, but the temperature de-

pendence, as a measure of the strength of pinning forces, is given by $(1 - t)^2$ instead of $(1 - t)^{3/2}$ - characteristic for materials with point-like defects. Measurements of the irreversible line H_{irr} in H_3S are desirable.

These columnar defects cause high density of the critical current and also a large magnetization hysteresis ΔM in H_3S . This property opens a possibility for making powerful high-field superconducting magnets. For instance, by making (if possible) a long superconducting cylinder of H_3S (with $L \gg R$) the magnetic hysteresis in that case is given by $\Delta M \sim j_{c0} \times R$, where R is the radius of the superconducting cylinder. For instance, in H_3S for $j_{c0} > 10^7$ A/cm² and for $R \sim 0.6$ cm one has $\mu_0 M \sim 100$ T at the temperature $T < 50$ K.

2. PMF in H_3S can be naturally explained by the SCPC model, where the strong columnar pinning of vortices dominates. The experiment measures PMF in the applied field $B_0 = \mu_0 H_0 = 0.68$ T [3]. If the field is penetrated in the center of the sample, then the quantum beats should appear in the ¹¹⁹Sn sensor. It turns out that in the perpendicular geometry, when the field is perpendicular to the sample surface ($B_0 \perp D$ - see Fig. 2), the magnetic field does not penetrate to the center, while in the parallel case ($B_0 \parallel D$ - see Fig. 2) it penetrates partially even for $T \ll T_c$ [3]. These experimental results are naturally explained in the SCPC model, where the “isotropically” distributed strong columnar pinning defects make a large current density $j_{c0}^\perp \approx j_{c0}^\parallel \approx (1.3 - 1.5) \times 10^7$ A/cm². It is also predicted, that the depinning temperature T_{dp}^r - where the critical current density is strongly weakened ($j_c(T) \ll j_{c0}$) and the field B_0 is fully penetrated into the H_3S sample, is of the order $T_{dp}^r \sim (100 - 120)$ K.

Moreover, in order to explain the TBR and PMF experiments by the SCPC model it comes out that H_3S is a high- κ superconductor with bulk physical parameters: $\xi_0 \approx (15 - 20)$ Å, $\lambda_0 \approx (1 - 2) \times 10^3$ Å; $\kappa \approx (50 - 100)$, $\mu_0 H_{c1}(0) \approx (18 - 60)$ mT, $\mu_0 H_{c0} \approx (0.6 - 1.1)$ T, $\mu_0 H_{c2} \approx (80 - 140)$ T. These values of parameters are also compatible with the microscopic theory of superconductivity. Finally, it is natural to raise the question - what is the origin of these columnar pinning defects in H_3S ? Serious candidates are single edge dislocations or their bundles, what is a matter of further research. To conclude - the SCPC model, which assumes the existence of strongly acting columnar pinning centers, is able to explain important TBR and PMF measurements in a high- κ H_3S superconductor. Therefore, there is no need for calling into question the existence of superconductivity in H_3S [10]-[13].

Acknowledgments

The author would like to thank Dirk Rischke and Radoš Gajić for permanent support and to Igor Kulić for discussions and support.

-
- [1] M. L. Kulić, arXiv:21.04.12214v1(2021)
- [2] M. I. Eremets et al, arXiv:2201.05137 (2022).
- [3] I. Troyan et al., *Science* **351**, 133 (2016)
- [4] A. Drozdov, M. Eremets, I. Troyan, V. Ksenofontov, S. Shylin, *Nature* **525**, 73 (2015)
- [5] M. Somayazulu, M. Ahart, A. K. Mishra, Z. M. Geballe, M. Baldini, Y. Meng, V. V. Struzhkin, and R. J. Hemley, *Phys. Rev. Lett.*, 122:027001, (2019); A. P. Drozdov, P. P. Kong, V. S. Minkov, S. P. Besedin, M. A. Kuzovnikov, S. Mozaffari, L. Balicas, F. F. Balakirev, D. E. Graf, V. B. Prakapenka, E. Greenberg, D. A. Knyazev, M. Tkacz, and M. I. Eremets, *Nature* **569**, 528, (2019)
- [6] D. V. Semenok et al., arXiv:2012.04787 (2020)
- [7] E. Snider et al., *Nature* **586**, 373 (2020)
- [8] E. Snider et al., *Nature* **586**, 373 (2020)D. Duan, Y. Liu, F. Tian, D. Li, X. Huang, Z. Zhao, H. Yu, B. Liu, W. Tian, T. Cui, *Sci. Rep.* 4, 6968; DOI:10.1038/srep06968 (2014)
- [9] N. Bernstein, C. Stephen Hellberg, M. D. Johannes, I. I. Mazin, M. J. Mehl, *Phys. Rev. B* **91**, R060511 (2015)
- [10] J. E. Hirsch. F. Marsiglio, *Phys. Rev. B* **103**, 134505 (2021); arXiv: 2101.01701 (2021)
- [11] J. E. Hirsch. F. Marsiglio, arXiv: 2103.00701v3 (2021)
- [12] J. E. Hirsch. F. Marsiglio, arXiv: 2110.07568v1 (2021);
- [13] J. E. Hirsch. F. Marsiglio, arXiv: 2110.07568v5 (2022)
- [14] V. S. Minkov et al, DOI:10.21203/rs.3.rs-936317/v1 (2021).
- [15] C. Bernhard, J. L. Tallon, E. Brücher, R. K. Kremer, *Phys. Rev. B* **61**, R14 960 (2000)
- [16] W. H. Jiao, H. F. Zhai, J. K. Bao, Y. K. Luo, Q. Tao, C. M. Feng, Z. A. Xu, G. H. Cao, *New Journal of Physics* **15**, 113002 (2013)
- [17] Yu. A. Genenko, S. V. Yampolskiib, A. V. Pan, *Applied Physics Letters* **84**, 3921 (2004)
- [18] L. Civale et al., *Phys. Rev. Lett.* **67**, 648 (1991)
- [19] G. Blatter et all, *Rev. Mod. Phys.* **66**, 1125 (1994)
- [20] G. S. Mkrtchyan, V. V. Schmidt, *Sov. Phys. JETP* **34**, 195 (1972)
- [21] M. L. Kulić, A. Krämer, K. D. Schotte, *Solid State Commun.* **82**, 541 (1992); A. Krämer, M. L. Kulić, *Phys. Rev. B* **48**, 9673 (1993); A. Krämer , M. L. Kulić, *Phys. Rev. B* **50**, 9484 (1994)
- [22] M. Tinkham, *Phys. Rev. Lett.* **61**, 1658 (1988)
- [23] P. W. Anderson, *Phys. Rev. Lett.* **9**, 309 (1962)
- [24] Y. Yeshurun, A. P. Malozemoff, *Phys. Rev. Lett.* **60**, 2202 (1988)
- [25] V. Ambegaokar, V. I. Halperin, *Phys. Rev. Lett.* **22**, 1364 (1969)
- [26] C. P. Bean, *Rev. Mod. Phys.* **36**, 31 (1964)
- [27] P. Mangin, R. Kahn, *Superconductivity An Introduction*, Springer (2017)
- [28] E. H. Brandt, *Phys. Rev. B* **58**, 6506 (1998)
- [29] J. E. Hirsch. F. Marsiglio, arXiv: 2109.10878v2 (2021)